Evaluating the Performance of Building Thermal Mass Control Strategies

James E. Braun, Ph.D. Member ASHRAE **Kent W. Montgomery** **Nitin Chaturvedi**

A tool was developed that allows evaluation of thermal mass control strategies using HVAC utility costs as the baseline for comparison. Inverse models are used to represent the behavior of the building, cooling plant, and air distribution system. Inverse models use measured data to "learn" system behavior and provide relatively accurate site-specific performance predictions. Based on weather and solar inputs, as well as occupancy and internal gains schedules and utility rates, the evaluation tool predicts the total HVAC utility cost for a specified control strategy. Intelligent thermal mass control strategies can then be identified in a simulation environment using this analysis tool. The evaluation tool was validated using data collected from a field site located near Chicago, Illinois. The tool predicted HVAC utility costs for a summer month billing period that were within approximately 5% of actual costs. Additional studies were performed to examine the utility savings potential for summertime operations at the field site using various thermal mass control strategies. The best strategy resulted in approximately a 40% reduction in total cooling costs as compared with night setup control. Simulation studies were also used to analyze the overall impact of location on the savings potential for use of building thermal mass. Representative utility rates for five locations (Boston, Chicago, Miami, Phoenix, and Seattle) were used along with the models obtained for the field site. Significant savings were achieved in all locations except Seattle.

INTRODUCTION

In order to reduce peak electrical demands, utilities provide price incentives for use of electricity during low demand or off-peak periods. One approach that customers may use to take advantage of these incentives involves cool thermal storage. The storage is cooled during off-peak periods when electricity is inexpensive and warmed during on-peak periods in order to reduce the load on the primary air conditioning equipment. Typically, ice and stratified chilled water systems are used as cool storage mediums. However, there is a significant extra cost associated with installing these systems. Furthermore, it is often difficult to retrofit an existing system with cool storage.

An alternative to ice or chilled water storage involves the use of the existing building structure for storage. With this scheme, the conventional cooling system is used to cool the air and structure during off-peak periods. Then, the zone temperatures are set to higher values during the on-peak period and the cooled structure acts to reduce heat gains to the air, leading to lower on-peak electrical requirements for air conditioning. Use of the building structure for thermal storage can provide significant load shifting with minimal initial cost for both new and existing buildings. It is only necessary to change the control strategy used for adjusting zone temperature setpoints.

Most buildings employ night setup control for zone temperatures, which does not take advantage of building thermal mass. During occupied hours, zone conditions are typically controlled

James E. Braun is a professor and **Nitin Chaturvedi** is a graduate student in the School of Mechanical Engineering, Ray W. Herrick Laboratories, Purdue University, West Lafayette, Indiana. **Kent W. Montgomery** is a business analyst with Ford Motor Company.

at constant set points that maintain acceptable comfort. During unoccupied times, the set points are raised, the equipment turns off, and the zone temperature is allowed to float. Night setup control strategies minimize the effects of building thermal storage. However, in many commercial buildings, the building mass has a significant thermal storage potential. An optimal controller might precool a building during the unoccupied period and control the storage discharge process by varying the setpoints within acceptable comfort bounds during occupancy.

There have been a number of simulation studies that showed significant reductions of operating costs in buildings by proper precooling and discharge of building thermal storage. The savings result from both utility rate incentives (time-of-use and demand charges) and improvements in operating efficiency due to night ventilation cooling and improved chiller performance (lower ambient temperatures and more even loading). Braun (1990) showed significant daily energy cost savings (10% to 50%) and peak power reductions (10% to 35%) over night setup control in a comprehensive simulation study that considered several building types and weather conditions. The daily percent savings were found to be most significant when low ambient temperatures allowed night ventilation cooling to be performed. Andresen and Brandemuehl (1992) simulated a typical zone of an office building and reported reductions in peak cooling loads of 10% to 50% depending on the control strategy that was used. Other simulation studies that yielded comparable results include Rabl and Norford (1991), Snyder and Newell (1990), and Golneshan and Yaghoubi (1990).

The simulation studies demonstrated that the savings potential and "best" control strategy are very dependent upon the system and particular weather conditions. Improper precooling can actually result in costs that are greater than those associated with conventional control. The importance of developing control strategies for each application has also been demonstrated through experimental evaluations.

Conniff (1991) used a test facility at the National Institute of Standards and Technology (NIST) to study the use of building thermal mass to shift cooling load. The facility was designed to represent a zone in a typical commercial office building. Several control strategies were considered in these tests. No attempt was made to optimize the control strategies for this facility. The most effective strategy tested for peak reduction did not employ precooling but used a constant zone temperature for the first seven hours of occupancy followed by a limit on the amount of cooling supplied to the zone. This strategy lowered the peak cooling demand by up to 15% of the lighting power when compared to night setup control. Other strategies that used precooling resulted in minimal cooling demand reductions (3%). Since thermal comfort was not evaluated during the tests, additional precooling may have been possible without sacrificing occupant comfort.

Ruud et al. (1990) performed two experiments on an office building located in Jacksonville, Florida. The control strategy called for cooling with a supply air temperature of 50°F (10°C) from 5 P.M. until 5 A.M. The first experiment resulted in several occupant comfort complaints that were addressed by adding a warm-up period just prior to building occupancy. No comfort complaints were reported after the warm-up period was initiated. The results showed 18% of the total daytime cooling load was shifted to the night period with no reduction in peak demand. Again, the control strategies used in that study were not optimized for that building.

Morris et al. (1994) devised and performed a set of experiments at the same facility used by Conniff (1991) in order to validate the potential for load shifting and peak reduction associated with optimal control. Prior to performing experiments, a simulation of the test facility was developed that included detailed models of the structure, cooling system, and comfort of a human occupant. Optimization techniques were applied to the simulation model in order to determine control strategies used in the two separate tests. The first control strategy was designed to minimize total energy costs and resulted in the shifting of 51% of the total cooling load to the off-peak hours. The second control strategy was designed to minimize the peak elec-

trical demand and resulted in a 40% reduction in peak cooling load. In both of these tests, data were collected to measure the occupant's thermal comfort. Thermal comfort was maintained within acceptable limits through both of the experiments. The results of Morris et al. (1994) were more encouraging than Conniff's (1991) for the same test facility because the control was optimized. Another important result of this work was the validation of the model used to develop the optimized control strategies. The hourly cooling loads from the building model closely matched the experimental results under both night setup and optimal control.

Keeney and Braun (1997) demonstrated a simple control strategy that makes use of building thermal mass in order to reduce peak cooling requirements in the event of a loss of a chiller. The control strategy was tested in a 1.4 million ft^2 (130 000 m^2) office building located near Chicago. The facility has two identical buildings with very similar internal gains and solar radiation loads that are connected by a large separately cooled entrance area. During tests, the east building used the existing building control strategy while the west building used the precooling strategy. Consistent with simulation predictions, the precooling control strategy successfully limited the peak load to 75% of the cooling capacity for the west building, while the east building operated at 100% of capacity. This same facility was used for results presented in the current paper.

Although the savings potential for use of building thermal mass has been demonstrated, very little work has been done in implementing effective control strategies in the field. One of the obstacles is the lack of available analysis tools for determining control strategies that are appropriate for a given field site. This paper presents a methodology for developing and evaluating building thermal control strategies for specific applications using limited field measurements. The methodology involves the use of inverse models for the building and plant that are trained with a limited amount of data from a field site. A system model is developed using the building and plant models along with a controller, weather data, and utility information. The tool is then used to evaluate costs associated with providing cooling in order to identify an appropriate control strategy for implementation. The methodology was developed for application to the field site used by Keeney and Braun (1997). However, it could be adapted to other facilities. More detailed information on the methodology and results presented in this paper appears in Montgomery (1998) and Chaturvedi (2000).

Test Facility

The field site is the headquarters for a large company and was commissioned for operation in 1990. It has a usable space of approximately 1.4 million ft^2 (130 000 m^2) with four stories (three above ground). The building has a large central reception area with office space consuming most of the remaining area (Figure 1). Office space is symmetrical on either side of the reception area. The building is constructed primarily of heavy weight concrete and has energy-efficient windows with excellent use of localized shading. The normal occupancy period for the facility is from 7 A.M. to 5 P.M., Monday through Friday. However, portions of the building are often occupied and conditioned after normal working hours.

The cooling plant for the building uses four 900-ton (3165-kW) centrifugal chillers. The chillers are paired on the east and west sides of the building. The system is configured so that both chiller pairs cooperatively cool the entire building. The chillers are controlled to maintain a constant chilled water supply setpoint. For each chiller's operation, there is a dedicated condenser water pump and chilled water pump. Both pumps use fixed-speed motors rated at 50 hp (37.3 kW). Heat rejection to the ambient is accomplished with two cooling towers, each containing three cells with two-speed fans. The motors driving the fans are rated at 50 hp (37.3 kW) for full-speed operation and 30 hp (22.4 kW) during low-speed operation. The system is configured so that each cooling tower serves a pair of chillers. Currently, the fans are controlled to maintain

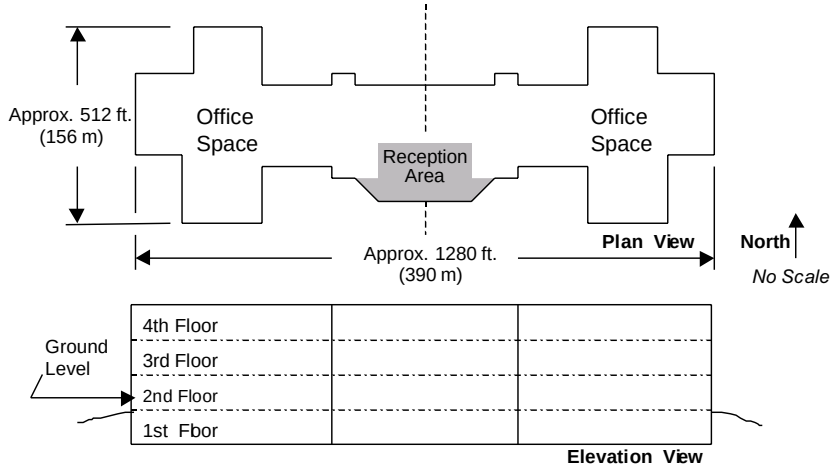

Figure 1. Layout of Field Site Building

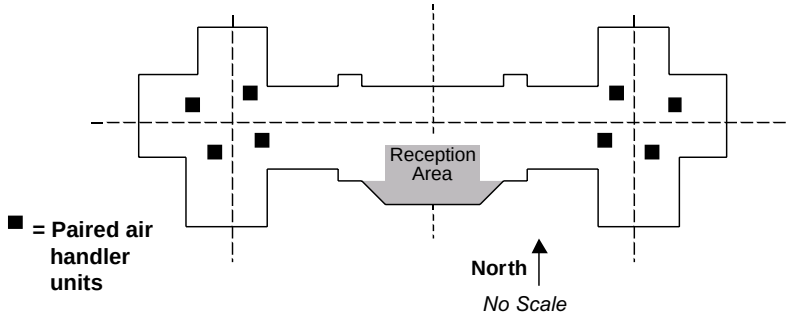

Figure 2. Plan View of Air Handling Unit Locations

a temperature setpoint in the cooling tower sump. The cooling plant provides chilled water to 16 air handling units (AHUs) within the building.

The 16 air handling units each contain one supply and one return variable-pitch, vane-axial fan. Each supply fan has a design flow rate of approximately 75,000 cfm (35 390 L/s). The return fans are designed for 70,000 cfm (33 030 L/s) each. The air handlers are paired in "quadrants" of the building so that each pair serves nearly equivalent areas. The power consumption meters record power data for each AHU pair. The approximate locations of the air handling unit pairs and the areas they serve are shown in Figure 2.

The air handler supply fans are controlled to maintain static pressure set points. The supply and return fans are linked, so that when one supply fan activates, one return fan also activates. Individual variable air volume (VAV) boxes located throughout the zones modulate airflow to maintain a zone temperature setpoint. Minimum fresh air requirements are maintained using outdoor air dampers.

The electric rates that were in place for summertime electrical energy usage at this facility when data were collected were \$0.05172/kWh on-peak (9 A.M. to 10 P.M.) and \$0.02273/kWh off-peak. The demand charge was \$16.41/kW (on-peak only) and was figured by averaging the peak usage over two 30-minute periods. The demand charge generally represents over 50% of the monthly energy bill for this facility.

Table 1. Data Points Recorded by the Energy Management System at the Field Site

Primary Component	Measured Values		
Building	• 8 Separate zone temperatures (4 on the 2nd floor and 4 on the 4th floor)	• Global building temperature setpoint	
Outdoor Environment	• Ambient temperature	• Ambient relative humidity	
Air Handlers (Typical of 8 pairs)	• Supply flow rate from AHU 1	• Supply flow rate from AHU 2	• Supply air temperature
	• Supply vane blade position for AHU 1	• Supply vane blade position for AHU 2	• On/Off status of AHU 1 supply fan
	• On/Off status of AHU 2 supply fan	• Return flow rate to AHU 1	• Return flow rate to AHU 2
	• Return air temperature	• Return vane blade position for AHU 1	• Return vane blade position for AHU 2
	• On/Off status of AHU 1 return fan	• On/Off status of AHU 2 return fan	• Supply static pressure setpoint
	• Supply static pressure	• Outdoor air damper positions	• Mixed return and outdoor air temperature entering the air handler
Chillers (Typical of 2 pairs)	• Unit 1 chill water supply temperature	• Unit 2 chill water supply temperature	• Combined chill water return temperature
	• Unit 1 chill water flow rate	• Unit 2 chill water flow rate	• Chiller bypass valve position
	• Unit 1 condenser water temperature to cooling tower	• Unit 2 condenser water temperature to cooling tower	• Combined condenser water temperature from cooling tower
	• Cooling tower cell 1 fan speed	• Cooling tower cell 2 fan speed	• Cooling tower cell 3 fan speed
	• On/Off status of unit 1	• On/Off status of unit 2	

The facility uses a computerized energy management to monitor and control the HVAC equipment and maintain zone conditions. Using this system, various measurements were recorded and averaged on an hourly basis for use in developing and validating simplified models. All individual measurements are recorded at 30-minute intervals. The data points recorded by the energy management system are listed in Table 1. The table is subdivided by the primary components measured: building, outdoor environment, air handlers, and chillers. The air handler data points are segregated by pairs because pairs of air handlers share a common supply and return duct. Each of the two chiller pairs also shares a common set of data points.

The sensible building cooling load and the total plant cooling load were necessary inputs for training the inverse building and plant models. These were calculated from the raw data with the following relationships. The sensible building cooling load is

$$\dot{Q}_{zs} = c_{p,a}\rho_a \sum_{i=1}^{8} [\dot{v}_{sup,pair,i}(T_{ret,i} - T_{sup,i})] \quad (1)$$

and the plant cooling load is

$$\dot{Q}_{plant} = c_{p,w}\rho_w \sum_{i=1}^{2} \{\dot{v}_{CHW,unit\ \#1,i}(T_{CHWR,i} - T_{CHWS,unit\ \#1,i}) + \dot{v}_{CHW,unit\ \#2,i}(T_{CHWR,i} - T_{CHWS,unit\ \#2,i})\} \quad (2)$$

The building temperature is a necessary input for training the simplified model. The representative building temperature was calculated by averaging eight zone temperatures recorded by the energy management system.

Electrical power data were obtained directly from the local utility company. Most of the building's HVAC electrical usage was divided between 12 meters: two for the chillers (one meter for each chiller pair), two for the pumps and auxiliaries, and eight for the air handlers (one meter per pair of air handlers). Total plant power was determined by adding the measured chiller power to estimated power requirements of the chilled water pumps, the condenser water pumps, and the cooling tower fans according to

$$P_{plant} = P_{ch} + N_{ch,on}(P_{CHW,pump} + P_{CW,pump}) + N_{ct,fan,on}P_{ct,fan} \quad (3)$$

The "on/off" statuses of each chiller and cooling tower fan were recorded. The chillers each have dedicated chilled water and condenser water pumps, such that they are sequenced on and off with the chillers. Individual pump and cooling tower fan powers were estimated from the data by the manufacturers.

Solar data were not measured directly at the field site, because the necessary equipment was not available. Instead, solar data collected from the St. Charles weather station were used. The St. Charles weather station is approximately 15 miles (24 km) southwest of the field site and is monitored by the Water and Atmospheric Resources Monitoring Program under the guidance of the Illinois State Water Survey. The St. Charles station uses an Eppley pyranometer to measure solar radiation. In addition to solar data, ambient temperature and relative humidity measurements were also available. The temperature and humidity measurements from this site were used for system simulations for the summer period.

Simulation Development

Figure 3 depicts the structure of the thermal mass simulation tool that was developed in this study. Thermal mass charging and discharging strategies are specified through hourly temperature setpoint schedules. The strategies are used along with occupancy internal gain schedules, weather data, utility rates, and the trained building, plant, and air handler models. The model performs hourly calculations to estimate monthly or seasonal cooling costs. At the end of each simulated month, a utility rate model is used to determine the total energy and demand charges. The utility cost data are written to a file, as are the number of comfort violations (in terms of zone temperature only) that occurred during the simulated month. This simulation tool can be used to evaluate utility costs for various thermal mass control strategies. In addition, the effects of weather, solar, and occupancy patterns on a particular strategy's operating cost can also be simulated using this tool for a specific building and cooling system.

The zone cooling requirement (or load) has both sensible and latent components. Latent gains are typically tied to the occupancy schedule and are relatively straightforward to estimate. On the other hand, the sensible gains are a complex function of the internal and external gains and the dynamic characteristics of the building structure. Sensible zone loads are due to heat transfer

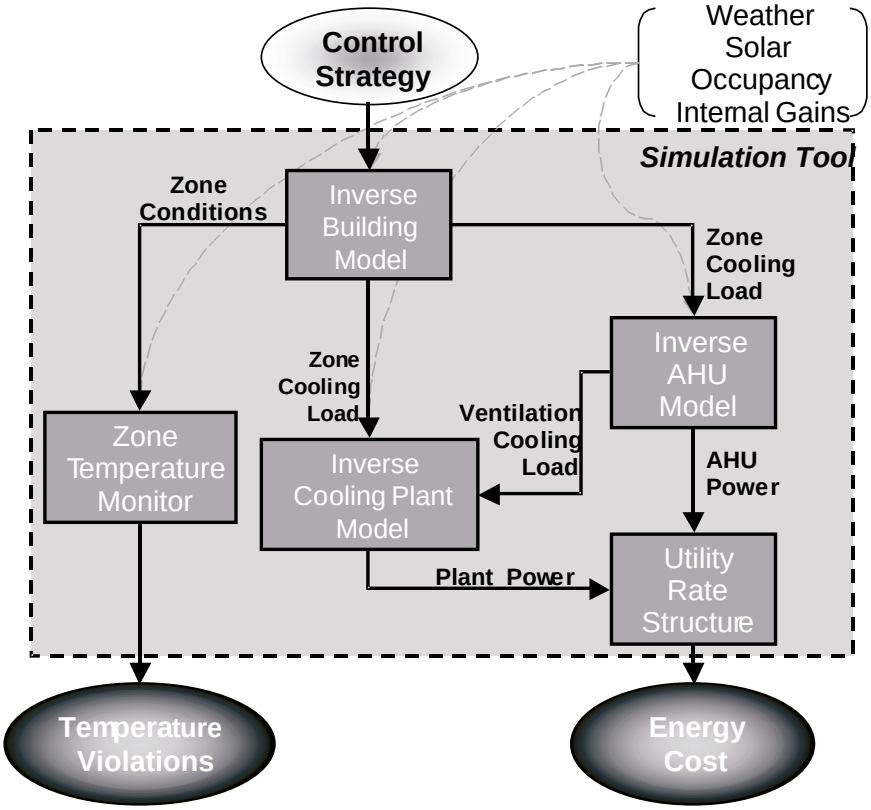

Figure 3. Overview of Thermal Mass Simulation Tool

from "warm" surfaces within the zone. Typical internal sources for heat gains are occupants, lights, and equipment (e.g., computers, copy machines, etc.). External sources for heat gains include solar radiation transmitted through windows and absorbed on external walls and energy conduction through external walls, and windows due to the difference between the ambient and space temperatures.

The inverse building modeling approach described by Chaturvedi and Braun (2002) was used to predict sensible cooling requirements for the building. The total heat gains to the air from the structure at any time *t* are determined using a transfer function of the form

$$\dot{Q}_{sh,t} = \sum_{k=0}^{8} \tilde{S}_k^T \tilde{u}_{t-k\Delta\tau} - \sum_{k=1}^{8} e_k \dot{Q}_{sh,t-k\Delta\tau} \tag{4}$$

The inputs include the zone temperature, ambient temperature, ground temperature, absorbed solar radiation on external surfaces, solar radiation transmitted through windows, and internal gains. Chaturvedi and Braun (2002) describe a robust method for determining the parameters of Equation (4). With a given set of parameters, Equation (4) can be used along with an energy balance on the air to estimate zone cooling requirements or zone temperatures.

If the air temperature is controlled at a constant temperature, then the sensible cooling requirement ($\dot{Q}_{zs}$) is equal to the heat gain ($\dot{Q}_{sh}$). However, if the cooling system is off, then the heat gains cause a change in the temperature and internal energy of the air and any other internal mass not considered within the building structure (e.g., furnishings). Energy storage within the internal mass also occurs when the cooling system is on and the zone temperature is changing (e.g., during precooling or when the setpoint is not achieved). In general, an energy balance on the internal mass gives

$$C_z \frac{dT_z}{dt} = \dot{Q}_{sh,t} - \dot{Q}_{zs,t} \tag{5}$$

where C_z is the capacitance associated with internal zone mass (air and furnishings).

In order to determine the sensible cooling requirements and zone temperature, three cases are considered: (1) zone temperature maintained at a constant set point, (2) zone temperature maintained at varying set points with specified initial and final values, and (3) floating temperatures with the cooling system off or providing a specified zone sensible cooling rate. In case 1, the left-hand side of Equation (5) is zero and the sensible cooling requirement is equal to the heat gain. The heat gain is evaluated with Equation (4) using average values of the input variables for each timestep. Thus, the cooling requirement represents an average value for the timestep.

In case 2, it is necessary to integrate Equation (5) over each timestep. In this case, the zone temperature is assumed to be linear over the timestep between the specified initial and final temperatures. Furthermore, the heat transfer gains are evaluated using the average zone temperature (and other inputs) over the timestep.

Case 3 occurs when the estimated cooling requirement for case 1 or 2 is less than zero (equipment turns off) or greater than a limit (the cooling capacity). In order to estimate the "floating" temperature, the heat gain is assumed to be constant and evaluated at the average zone temperature over the timestep and the zone sensible cooling rate is a constant (zero or a maximum capacity). This assumption leads to a linear variation in the zone temperature and the average and final temperatures are determined from Equations (4) and (5) as

$$\bar{T}_{z,t} = \frac{\sum_{l=2}^{9} \hat{S}_0(l)\hat{u}_t(l) + \sum_{j=1}^{8} \hat{S}_j^T \hat{u}_{t-j\Delta\tau} - \sum_{j=1}^{8} e_j \dot{Q}_{sh,t-j\Delta\tau} - \dot{Q}_{zs,t} + 2\frac{C_z}{\Delta\tau} T_{z,t-\Delta\tau}}{2\frac{C_z}{\Delta\tau} - \hat{S}_0(1)} \tag{6}$$

$$T_{z,t} = T_{z,t-\Delta\tau} + 2\bar{T}_{z,t} \tag{7}$$

where $\hat{S}_0(l)$ is the l^{th} element of the $\hat{S}_0$ vector.

Occupant comfort is monitored using the hourly zone air temperatures. A minimum and maximum allowable zone air temperature is specified for occupied periods. Comfort conditions are not considered during unoccupied periods. The comfort monitor keeps track of the number of air temperature violations for each month during the simulation period.

The power consumption of an air handler fan can primarily be correlated with airflow rate. In this study, the following functional form was found to work well:

$$P_{ahu,pair} = a_0 + a_1 \dot{v}_{sup,pair} + a_2 \dot{v}_{sup,pair} \tag{8}$$

The coefficients of Equation (8) are estimated using linear regression applied to measurements of flow and power consumption.

For the facility considered in this study, the 16 AHUs are identical and have approximately the same number of operational hours since the original commissioning of the building. In addition, because of the building's symmetry, the supply airflow rates for the eight AHU pairs are nearly identical. Assuming that the performance characteristics of the paired units are identical and equally distributed airflow to all AHUs, the total AHU power is calculated as

$$P_{ahu,total} = N_{ahu,pairs} P_{ahu,pair} \tag{9}$$

The volumetric flow rate for each AHU pair is

$$\dot{v}_{sup,pair} = \frac{\dot{v}_{sup}}{N_{ahu,pairs}} \tag{10}$$

Based on the sensible zone load, the building supply air mass flow requirement is

$$\dot{m}_{sup} = \frac{\dot{Q}_{zs}}{c_{p,a}(T_z - T_{sup})} \tag{11}$$

The ventilation cooling load is necessary for estimating the plant cooling load and is calculated as

$$\dot{Q}_{vent} = \dot{m}_{vent}(h_a - h_z) \tag{12}$$

The ventilation flow rate depends upon the ventilation strategy employed. The model assumes that the zone air relative humidity is fixed for the zone air enthalpy calculation in the above relation. In order to consider a floating zone humidity, it would be necessary to include a cooling coil model. However, it is expected that the impact of a floating humidity ratio on comparisons between control strategies would be relatively small.

The total cooling plant load and corresponding power requirement are determined by the cooling plant model. The total cooling load is calculated as

$$\dot{Q}_{plant} = \dot{Q}_{zs} + \dot{Q}_{zl} + \dot{Q}_{vent} \tag{13}$$

The zone latent load ($\dot{Q}_{zl}$) is the energy rate that would be required to remove (i.e., condense) the moisture gains from the zone and are primarily due to occupants.

The total cooling plant load is assumed to be divided equally among the active chillers. An additional chiller is activated when the primary chiller reaches a set percentage of its maximum operational power consumption and maintains or exceeds that load for a defined time period. A number of different model forms were considered for mapping the cooling plant power consumption. The following quadratic form was found to work well:

$$
\begin{aligned}
P_{plant} = {} & a_0 + a_1 N_{ch,on} + a_2 \sum_{i=1}^{N_{ch,on}} \dot{Q}_{ch,i} + a_3 \left(\sum_{i=1}^{N_{ch,on}} \dot{Q}_{ch,i} \right)^2 + a_4 N_{ch,on} T_{wb} \\
& + a_5 N_{ch,on} T_{wb}^2 + a_6 \sum_{i=1}^{N_{ch,on}} T_{chws,i} + a_7 \left(\sum_{i=1}^{N_{ch,on}} T_{chws,i} \right)^2 \\
& + a_8 \sum_{i=1}^{N_{ch,on}} \dot{Q}_{ch,i} \sum_{i=1}^{N_{ch,on}} T_{wb,i} + a_9 \sum_{i=1}^{N_{ch,on}} \dot{Q}_{ch,i} \sum_{i=1}^{N_{ch,on}} T_{chws,i} \\
& + a_{10} N_{ch,on} T_{wb} \sum_{i=1}^{N_{ch,on}} T_{chws,i}
\end{aligned} \tag{14}
$$

The individual chiller is simply the plant load divided by the number of active chillers. The coefficients of Equation (14) are determined by applying linear regression given measured plant power consumption, plant cooling loads, chilled water set points, and ambient wet-bulb temperatures. Since this model does not incorporate the cooling tower and pump controls, it assumes that the control strategies for these devices do not change. Therefore, it would not allow extrapolation to new cooling tower and/or pump control strategies.

During operation, the cooling plant and air handler fans have limited capacity that must be considered. In addition, there may be lower limits on capacity to ensure safe equipment operation.

If the required air handler fan flow rate is greater than the fan capacity, then the zone temperature can no longer be maintained. In this case, the fan flow is set to its maximum value and a floating zone temperature is determined that satisfies an energy balance on the internal zone mass (air plus furnishings). Similarly, if the fan flow is less than a lower limit, then the fan flow is set to its lower limit and a floating temperature is determined. In either case, the energy balance on the internal zone mass can be written as

$$
\begin{aligned}
C_z \frac{dT_z}{dt} = {} & \sum_{l=2}^{9} \vec{S}_0(l) \vec{u}_t(l) + \sum_{j=1}^{8} \vec{S}_j^T \vec{u}_{t-j\Delta\tau} - \sum_{j=1}^{8} e_j \dot{Q}_{sh,t-j\Delta\tau} \\
& + \vec{S}_0(1) T_z - \dot{m}_{sup} c_{p,a} (T_z - T_{sup})
\end{aligned} \tag{15}
$$

where $\vec{S}_0(l)$ is the l^{th} element of the $\vec{S}_0$ vector.

Equation (15) is a first-order differential equation in zone temperature that is integrated analytically over each timestep. The average zone temperature over the timestep is then used to evaluate the average heat gains and cooling requirements according to

$$
\dot{Q}_{sh,t} = \sum_{l=2}^{9} \vec{S}_0(l) \vec{u}_t(l) + \sum_{j=1}^{8} \vec{S}_j^T \vec{u}_{t-j\Delta\tau} - \sum_{j=1}^{8} e_j \dot{Q}_{sh,t-j\Delta\tau} + \vec{S}_0(1) \bar{T}_z \tag{16}
$$

$$
\dot{Q}_{zs} = \dot{m}_{sup} c_{p,a} (\bar{T}_z - T_{sup}) \tag{17}
$$

If total plant cooling load exceeds the maximum plant capacity or is less than a minimum, then the zone temperature set point can no longer be maintained. In this case, the total cooling load is set equal to the limiting value (maximum or minimum value) and the zone temperature that achieves this constraint along with the other equations is determined iteratively.

The model uses the site utility rate structure in conjunction with the total HVAC power requirement to determine the total HVAC utility costs as follows:

$$P_{tot,i} = P_{plant,i} + P_{AHU,i} \tag{18}$$

$$C_{tot} = \sum_{i=1}^{N_{on}} (P_{tot,i} R_{on,peak}) + \sum_{i=1}^{N_{off}} (P_{tot,i} R_{off,peak}) + Max_{i=1,2,\ldots,N_{on}} (P_{tot,i}) R_{demand,on} \tag{19}$$

Model Training and Testing

Approximately six weeks of hourly data from the summer of 1997 were available from the energy management system for training and testing the building model, whereas only about four weeks of coincident detailed electrical data were obtained from the local utility for training the plant and air handling unit models. Coincident solar data were available from the St. Charles measurement site.

The modeling and training approach described in detail by Chaturvedi and Braun (2002) was applied to the data from the field site. Two weeks of data were used for training, while four weeks were used to test the model. Training involved determining the parameters of Equation (4) that minimized errors in the hourly predictions of the zone sensible load. The zone capacitance was estimated from a description of the building and was not adjusted during the training process.

It was necessary to make assumptions for some of the unmeasured inputs for both training and testing of the simplified model. The control strategy in place was a light precooling strategy. However, the set point was not always maintained, so the measured temperature (calculated as the average of the eight measured building temperatures) was used to train and test the simplified model. Internal gains were modeled as a combination of the sensible gains from the occupants and the lighting and equipment. The occupant gains were calculated using a fixed number of occupants (3500), each with a heat loss of 75 W (ASHRAE 1997). The lighting and equipment gains were estimated to be 5 W/ft^2 in the occupied period. The total internal gains were assumed to be 70% radiative and 30% convective. The unoccupied period internal gains were taken to be 10% of the total occupied period gains. The occupied period was taken to be from 7 A.M. to 5 P.M. on weekdays.

A sensitivity study was carried out to evaluate the impact of changes in model performance with changes in different parameters. It was found that the model errors were most sensitive to the magnitude of the internal gains. This is not surprising, since large buildings are generally dominated by internal gains. Furthermore, internal gains were not well known, especially during unoccupied times. Three additional parameters were introduced in the model to tune the internal gains schedule. The three parameters were multiplying factors applied to the estimated occupied period gains during occupied, unoccupied, and weekend periods.

Comparisons of measured and predicted load and zone temperatures are shown in Figure 4 and Figure 5. Zone loads were predicted under the given temperatures and zone temperatures were estimated during periods of floating temperature. The model does an excellent job of predicting the trends in the transient variations. Generally, the hourly load predictions are within 10% of the actual values and the zone temperatures are within 1°F (0.56°C).

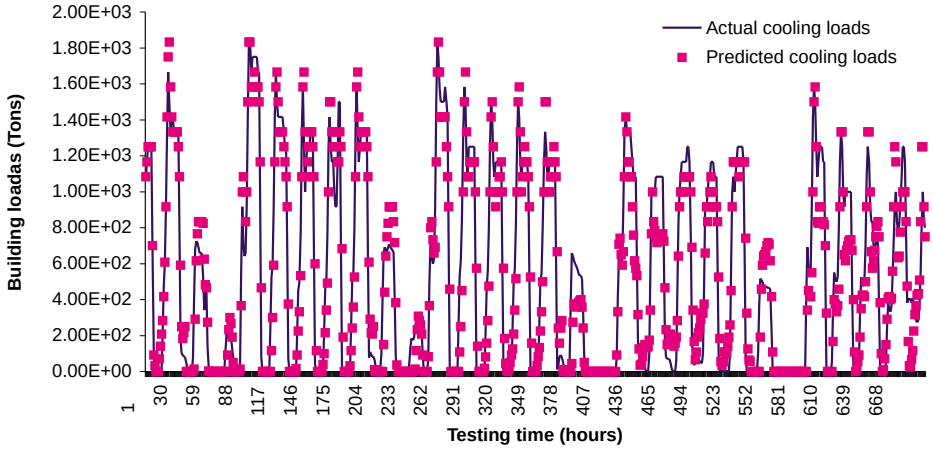

Figure 4. Comparison of Actual and Predicted Sensible Cooling Loads for Testing Period (14 Days Training)

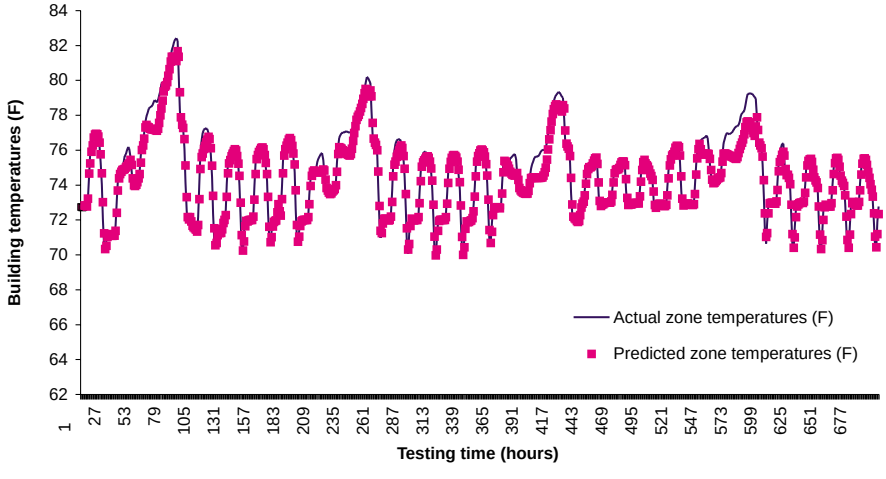

Figure 5. Comparison of Actual and Predicted Zone Temperatures for Testing Period (14 Days Training)

Electric and flow rate data were available for five individual AHU pairs. A total of 660 data points were available for each AHU pair. Linear regression was applied to fit coefficients of Equation (8) for a single AHU pair, and then the model was tested using data for the other AHU pairs. Figure 6 demonstrates the accuracy of the model for the training data. Figure 7 and Figure 8 show the model power predictions associated with test data from two other AHUs. The RMS errors for these two other cases were 23.79 kW and 22.24 kW, respectively. In general, the model is adequate for predicting the effect of airflow on AHU power.

The parameters of Equation (14) were estimated for the field site using linear regression applied to data recorded from July 10 to July 28, 1997. Figure 9 shows comparisons between predicted and measured plant power consumption for the training data. For these data, the R^2

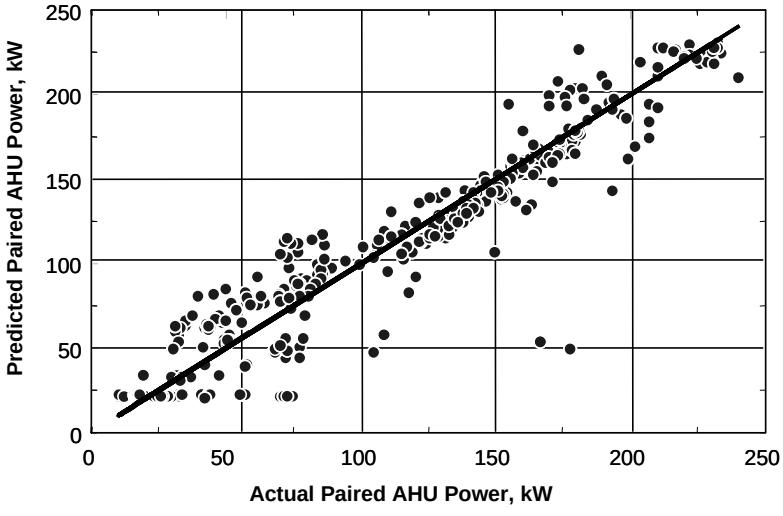

Figure 6. AHU vs. Actual Power (Training Data)

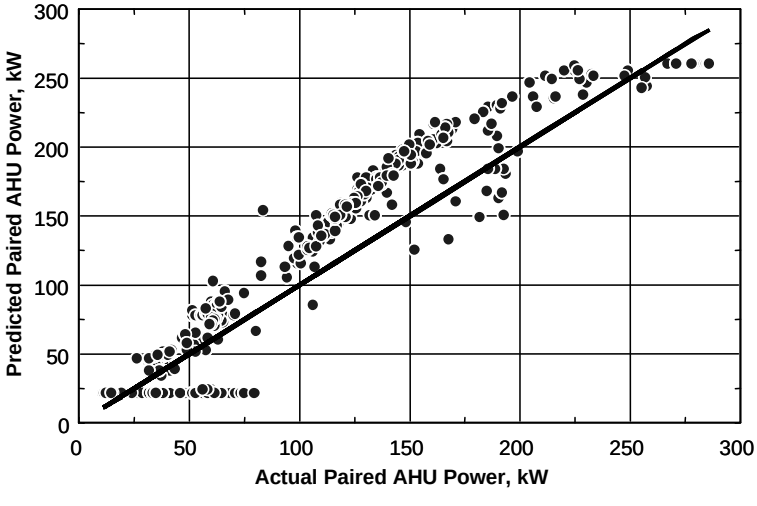

Figure 7. AHU Model vs. Actual Power (1st Set of Test Data)

value was 0.9792 and the calculated RMS prediction error was 107.4 kW. The model also predicts the correct trends of increasing power with decreasing chilled water temperature and increasing wet-bulb. Overall, the model is adequate for estimating plant power consumption for the purpose of comparing different zone control strategies.

Simulation Tool Validation

Approximately one month's data recorded at the field site were used to compare predicted HVAC utility costs with an actual site utility bill.

A utility bill for the facility was obtained that was dated August 11, 1997. The billing period for this statement began July 9, 1997, and concluded August 7, 1997. The billing statement was structured such that meters associated with HVAC energy usage were presented separately from

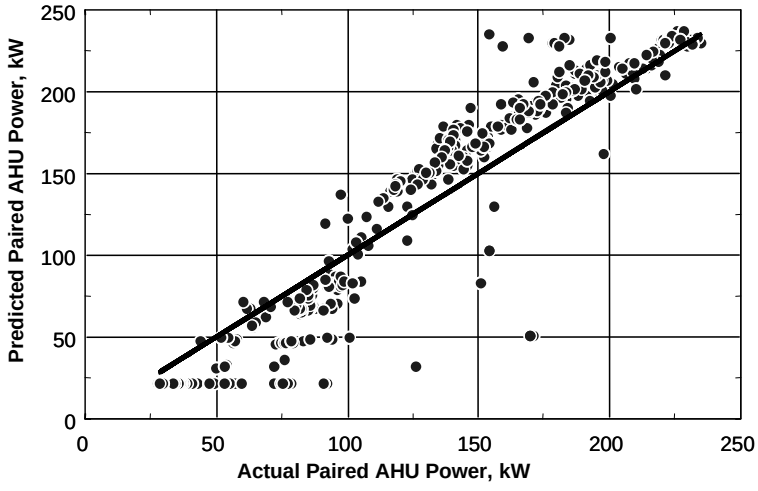

Figure 8. AHU Model Predictions vs. Actual Power (2nd Set of Test Data)

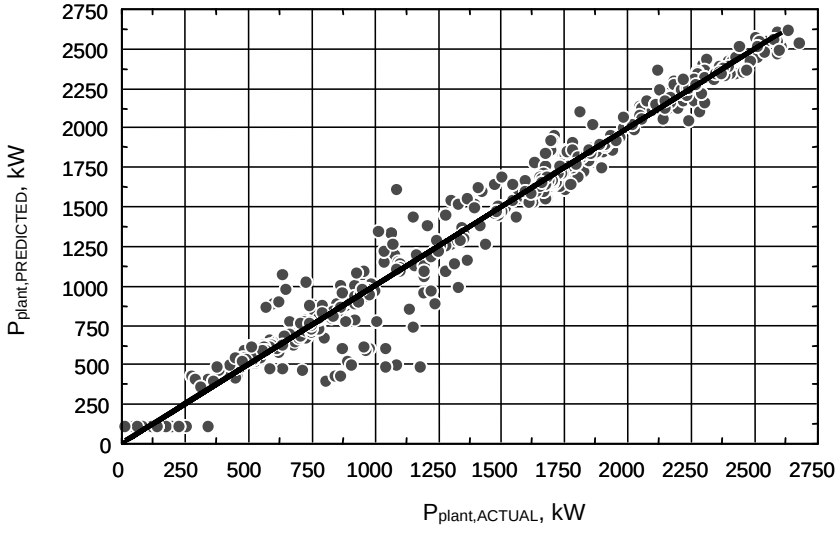

Figure 9. Model Predictions vs. Actual Power for Plant

other general usage meters. In addition, the total energy usage, the off-peak energy usage, and the demand usage for each meter were detailed. The HVAC utility charges were about half of the total utility bill for this period, whereas the total demand charge accounted for 55% of the total utility bill.

The total HVAC-related utility charges for the August 11, 1997 statement were $120,012, with $73,264 (or 61%) for demand and $46,748 (or 39%) for energy charges. The on-peak HVAC energy charges accounted for 28% of the total HVAC costs and nearly 72% of the total HVAC energy charges. The HVAC utility costs could be further broken down with 45% for the chillers, 37% for the air handling units, and 18% for additional HVAC auxiliaries (pumps and cooling tower fans).

Data collected from the facility were used in conjunction with the simulation tool to predict utility costs for the purpose of model validation. Because the data collection period did not begin

until noon on July 10, 1997, the exact billing period could not be duplicated. Instead, the data used for the simulated billing period began at midnight July 11 and lasted until midnight, August 9, 1997. However, the same number of days was simulated with the same ratio of weekday to weekend hours.

The coefficients used for the inverse building, plant, and AHU models were determined by training each model on all available data. Thus, the inverse building model was trained using the 41 days of available building data, and the coefficients for the inverse plant and AHU models were determined from the 660 hourly data points recorded during the summer of 1997.

The internal gain schedule defined and tuned during the building modeling process (Chaturvedi and Braun 2002) was used in the simulation tool validation and application. During unoccupied periods, the outdoor air ventilation was set to zero. If the building was occupied, it was assumed that the total supply airflow was composed of 25% outside air and 75% return air from the zones. An economizer mode was not operational during this period. The zone relative humidity was assumed constant at 50% and the supply air temperature to the zone was held constant at 55°F (12.8°C) In this study, the building occupants were assumed to be the only source of building latent gains. Each occupant was assumed to have a latent gain of 255 Btu/h (74.7 W).

The plant model requires a chiller staging scheme for plant power estimates. During the test period, staging and operation of the east side chillers were independent of the west side and vice versa. Overall efficiency could be increased through global staging of all four chillers. To represent the inefficient chiller staging scheme used during the summer of 1997, the staging scheme given in Table 2 was used.

The actual zone control strategy in use at the field site for the majority of the utility billing period was a light precooling strategy that began precooling at 3 A.M. However, the system was not operating properly and the zone temperature setpoints were not maintained during the precool period. As a result, the actual zone temperature measurements were used as setpoints in the validation of the model. This is consistent with the strategy used for training the building model as described by Chaturvedi and Braun (2002).

The results of the validation exercise are presented in Figure 10. The simulation tool underpredicted the total HVAC bill by about 5%. The relative errors were higher for the energy portion of the bill than for the demand charges. This may be due to difficulties in modeling the actual chiller staging and unanticipated after-hour cooling requirements. Both of these effects would tend to increase energy costs during unoccupied times. The model certainly works well enough to be used in comparing the performance of alternative control strategies and studying the effects of climate and utility rates.

Evaluation of Control Strategies

The validated simulation tool was used to estimate cooling season operating costs for a variety of strategies, utility rates, and locations. For these simulations, typical meteorological year (TMY) data were used for all locations. A more efficient chiller staging scheme defined in Table 3 was used for all of the simulations. The simulation tool predicted about a 10% costs savings associated with this strategy compared with the strategy of Table 2. The minimum loading for a single chiller was set at 200 tons. The acceptable range of occupied zone air temperatures was considered to be between 69°F to 77°F (20.6°C to 25°C). This range was based on comfort

Table 2. Chiller Staging Scheme Used for Model Validation

Total Cooling Load	Number of Active Chillers
1-800 tons (3.5 to 2800 kW)	2
800-3600 tons (2800 to 12 600 kW)	4

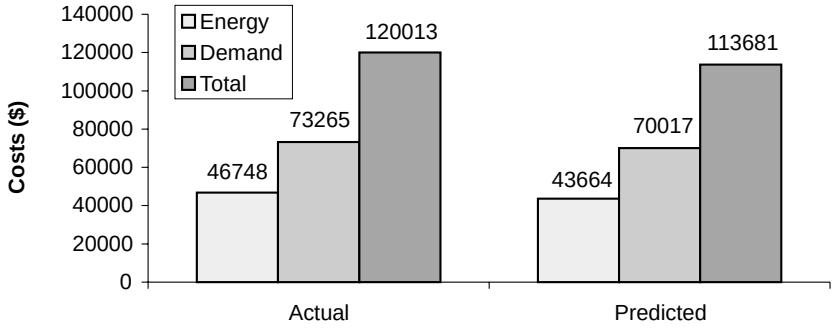

Figure 10. Comparison of Actual and Simulation Tool Predicted HVAC Utility Costs (July 11–August 8, 1997)

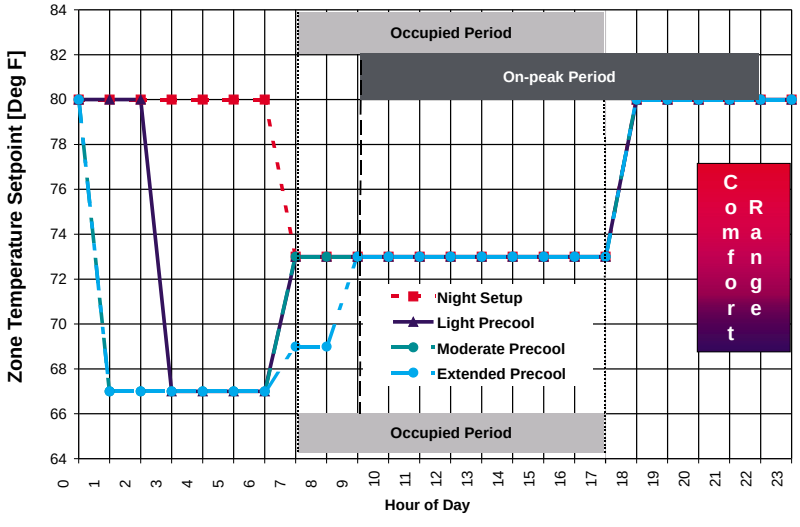

Figure 11. Weekday Hourly Zone Temperature Setpoint Definitions for Night Setup, Light Precool, Moderate Precool, and Extended Precool Strategies

Table 3. Definition of Efficient Chiller Staging Scheme Used for Simulation Studies

Total Cooling Load	Number of Active Chillers
1 to 800 tons (3.5 to 2800 kW)	1
800 to 1700 tons (2800 to 5600 kW)	2
1700 to 2400 tons (5600 to 8400 kW)	3
2400 to 3600 tons (8400 to 12 600 kW)	4

studies specific to the field site performed by Keeney and Braun (1997). An economizer mode was not considered, and precooling was only accomplished using mechanical cooling.

Several thermal mass precooling and discharge strategies were examined for utility cost reduction potential at the field site. Figure 11 shows zone setpoint temperature variations for four strategies where the on-peak, occupied setpoint was held constant at 73°F (22.8°C). Night

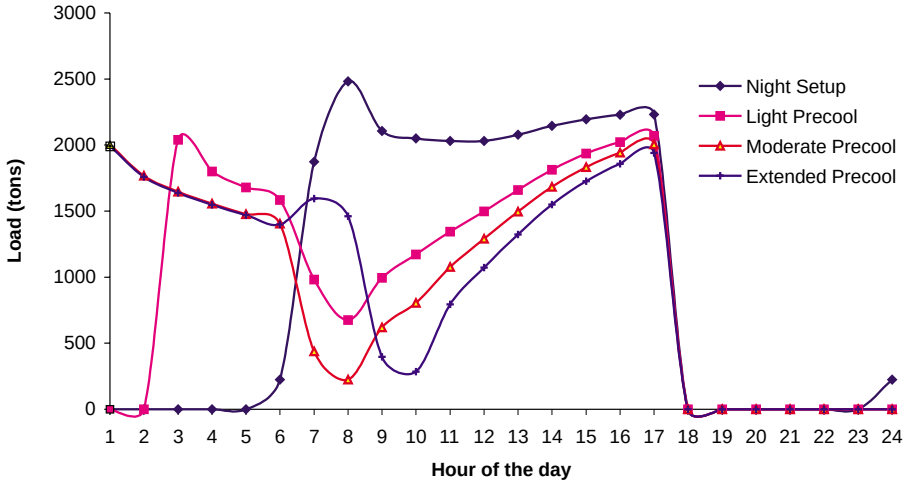

Figure 12. Plant Cooling Load Profiles for Night Setup, Light Precool, Moderate Precool, and Extended Precool Strategies

setup was the baseline used for comparing the alternative strategies. The light precool and moderate precool strategies are simple strategies that precool the building at a fixed setpoint of 67°F (19.4°C) prior to the onset of occupancy and then maintain a fixed discharge setpoint in the middle of the comfort range, 73°F (22.8°C), during occupancy. The light precool begins at 3 A.M., whereas moderate precool starts at 1 A.M. The extended precool strategy attempts to maintain the cooled thermal mass until the onset of the on-peak period. In this case, the setpoint at occupancy is maintained at the lower limit of comfort, 69°F (20.6°C), until the on-peak period begins at 9 A.M. At this point, the setpoint is raised to the middle of the comfort range, 73°F (22.8°C).

Figure 12 shows the simulated cooling plant loads for a sample day in the middle of July in Chicago for each of the strategies. Night setup resulted in very little cooling during the unoccupied period and a peak requirement in the early morning. The cooling requirement was relatively flat during the day, with a second peak near the end of the occupied period. Each of the precool strategies resulted in reduced cooling requirements throughout the occupied period, but particularly in the early morning. The greater the precooling, the greater the on-peak period load reduction. Although the on-peak total cooling requirement was reduced significantly for each strategy, the peak cooling requirement during the on-peak period was only marginally reduced: these strategies tend to discharge the mass relatively early during the on-peak period.

The peak loads can be reduced further if the entire comfort range is used throughout the on-peak, occupied period. Figure 13 shows two additional strategies that have the same precooling characteristics as the extended precool strategy, but that use the entire comfort range during the on-peak, occupied period. The maximum discharge strategy attempts to discharge the mass as quickly as possible following the onset of the on-peak period. In this case, the setpoint is raised to the upper limit of comfort within an hour after the on-peak period begins. The maximum discharge strategy maximizes storage efficiency and load shifting, but is not necessarily optimal in terms of peak load reduction. It tends to lead to low loads during the morning and a peak during the late afternoon. Linear rise strategies were also investigated as a means of leveling the load in order to reduce the peak loads further. The slow linear rise strategy raises the setpoint linearly over the entire on-peak, occupied period (nine hours in this case), whereas the fast linear rise strategy raises the setpoint over four hours.

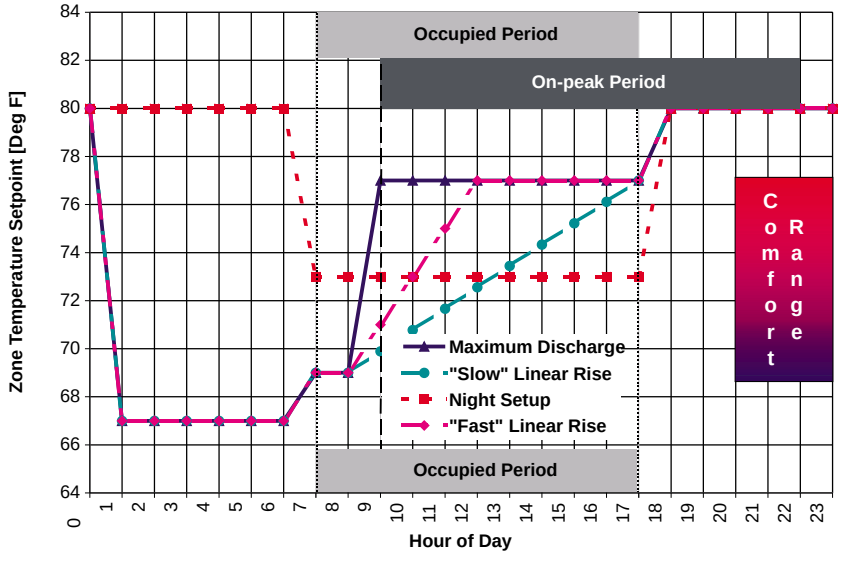

Figure 13. Weekday Hourly Zone Temperature Setpoint Definitions for Night Setup, Maximum Discharge, and Linear Temperature Rise Strategies

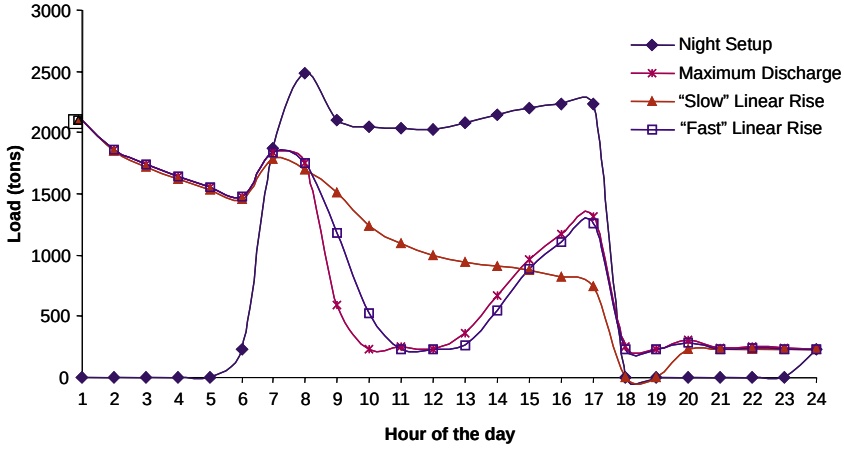

Figure 14. Plant Cooling Load Profiles for Night Setup, Maximum Discharge, and Linear Rise Strategies

Figure 14 shows cooling load profiles for the strategies of night setup, maximum discharge, and linear rise for the same day in July. The maximum discharge strategy results in the lowest on-peak total load. It also has a slightly lower peak load than the linear rise strategies during the on-peak period (after 9 A.M.). The fast linear rise strategy has a flatter on-peak load profile, but has its peak at the onset of the on-peak period. It is interesting to note that both maximum discharge and fast linear rise strategies result in minimum chiller loading at the onset of the on-peak period.

The simulation tool was run for a three-month period (June to August) to estimate the savings potential of the different control strategies for the field site. Table 4 shows the energy, demand

Table 4. Cooling Season Energy, Demand, and Total Costs and Savings Potential of Different Control Strategies (Chicago)

Strategy	Energy Costs, $	Demand Costs, $	Total Costs, $	Savings, %
Night setup	90,802	189,034	279,836	0.0
Light precool	84,346	147,581	231,928	17.1
Moderate precool	83,541	143,859	227,400	18.7
Extended precool	81,715	134,551	216,266	22.7
Maximum discharge	72,638	91,282	163,920	41.4
Two-hour linear rise	72,671	91,372	164,043	41.4
Four-hour linear rise	73,779	115,137	188,916	32.5
Nine-hour linear rise	77,095	141,124	218,219	22.0

Table 5. Comparison of Current and Less Favorable Utility Pricing Schemes

Description	Current	Less Favorable
Off-peak energy, $/kWh	0.023	0.0268
On-peak energy, $/kWh	0.052	0.0388
Off-peak demand, $/kWh	0	0
On-peak demand, $/kWh	16.41	5.6
On-to-off peak ratio	2.3	1.4
Peak period	9 A.M. to 10 P.M.	9 A.M. to 10 P.M.

and total utility costs. The savings in Table 4 are relative to night setup as a baseline. Three different linear rise strategies were investigated.

The strategies that do not utilize the entire comfort range during the occupied period (light precool, moderate precool, and extended precool) all provided about 20% savings relative to night setup. Each of these strategies reduced both energy and demand costs. However, the demand costs and demand cost reductions were significantly greater than the energy costs and savings. The decreases in energy costs were due to favorable on-to-off peak energy rate ratios of about 2 to 1. The high on-peak demand charges provided even greater incentives for use of precooling. The savings increase with the amount of precooling period, particularly when the precooling is performed close to the onset of on-peak rates.

The maximum discharge strategy, which maximizes discharge of the thermal storage within the structure, provided the largest savings (41%). Much of the additional savings was due to reductions in the demand costs. The linear rise strategies also provided considerable savings; the faster the linear rise in setpoint temperature, the greater the savings.

The utility for the field site has a very favorable rate structure for implementing thermal mass strategies. However, rate structures vary widely, even within one region of the country. For comparison, another rate structure for the midwestern United States region was investigated. This structure had the lowest demand charges and the lowest on-to-off peak ratio (least favorable rates) among all the investigated utility rate structures in the midwestern United States.

Table 5 shows the current (favorable structure) and the less favorable utility rate structure. Both structures have the same on-peak periods (9 A.M. to 10 P.M. between Monday and Friday) with all other periods and holidays on off-peak rates.

Table 6 shows energy, demand, and total costs for the less favorable rates for the cooling season in Chicago, along with percent savings relative to night setup. For these rates, the demand costs were less than the energy costs for all strategies. However, the savings were still primarily

Table 6. Energy, Demand, and Total Costs and Percent Savings for Different Control Strategies with Less Favorable Utility Rates (Chicago)

Strategy	Energy Costs, $	Demand Costs, $	Total Costs, $	Savings, %
Night setup	74,370.0	64,509.0	138,879.0	0.0
Light precool	74,645.0	50,363.0	125,008.0	10.0
Moderate precool	76,750.0	49,093.0	125,843.0	9.4
Extended precool	76,926.0	45,916.0	122,843.0	11.5
Maximum discharge	71,921.0	31,150.0	103,071.0	25.8
Slow linear rise	74,386.0	48,159.0	122,545.0	11.8

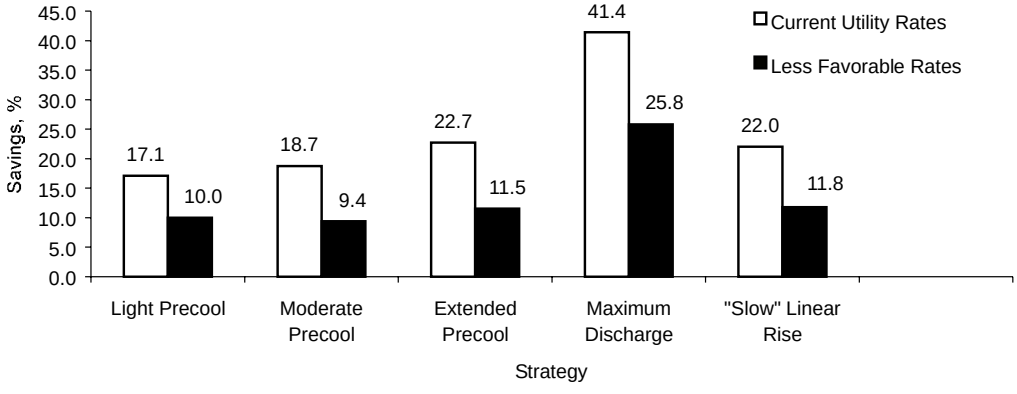

Figure 15. Comparison of Savings Potential of Different Control Strategies Under Current and Less Favorable Utility Rates (Chicago)

due to demand cost reductions. In fact, the strategies that maintain fixed set points during the on-peak, occupied period (light precool, moderate precool, and extended precool) actually had slightly higher energy costs than night setup, with greater penalties associated with greater precooling. Precooling caused an increase in the total cooling load that offset any energy cost savings associated with load shifting. However, these strategies still saved about 10% in total costs relative to night setup.

The savings for the maximum discharge strategy were still significant (25%) for the less favorable utility rate. Both energy and demand costs were reduced. The energy costs are less than the other precool strategies because the fast discharge leads to higher storage efficiencies. The savings associated with the slow linear rise (nine hours) were comparable to the extended precool strategy.

Figure 15 presents a graphical comparison of savings associated with the two utility rate strategies for the field site. The savings were reduced by a factor of about 1.5 to 2.0 for each strategy with the less favorable structure. However, the savings are still significant.

The models of the existing building, cooling system, and utility rates were used to investigate the effect of climate on the savings potential of building thermal mass control strategies. The combination of utility and climate effects is presented in the next section. Five representative cities for different regions of the United States were investigated: Boston, Massachusetts; Chicago, Illinois; Miami, Florida; Phoenix, Arizona; and Seattle, Washington.

Boston, Chicago, and Seattle represent cities with cooler to moderate ambient temperatures and moderate incident solar radiation. Miami and Phoenix have much higher average ambient

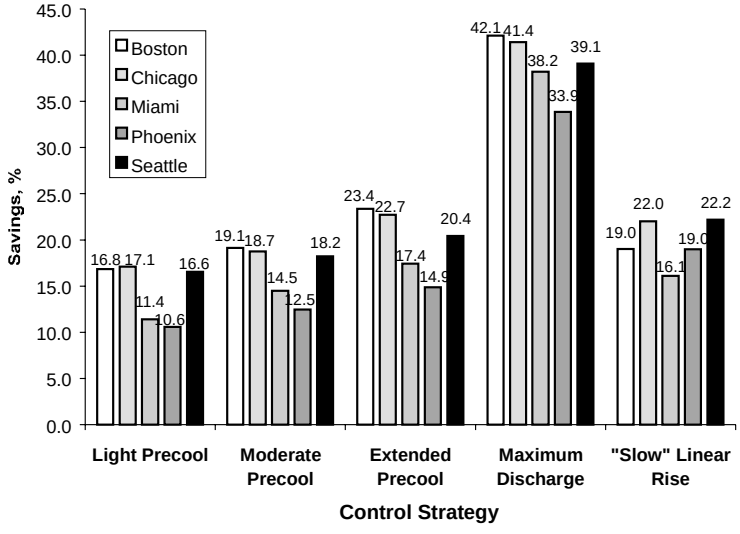

Figure 16. Comparison of Savings Potential of Different Control Strategies Under Different Climatic Conditions (Chicago Utility Rate Structure)

temperatures and higher incident solar radiation. Phoenix has a relatively dry climate, while Miami represents more humid ambient conditions.

Figure 16 shows the effect of climate on the air conditioning cost savings for different control strategies. All of the control strategies led to significant savings in all of the locations for the favorable rate structure associated with the field site. However, more temperate climates such as those of Boston, Chicago, and Seattle resulted in larger relative savings (5 to 10%) than climates with high ambient temperatures and high incident solar radiation (Miami and Phoenix). There may be a couple of effects that are important in explaining these differences. First, conduction gains through walls and windows are a more significant fraction of the total loads in warmer climates. Since precooling results in a larger temperature difference for envelope gains, the overall building storage efficiency will be lower in warmer climates. Second, the amount of precooling associated with any of the strategies is relatively fixed, since the precool temperatures and time periods are fixed. Thus, the quantity of load shifting is a smaller percentage of the total load for climates that result in higher baseline loads.

The test building is somewhat typical of large multi-story buildings in that the loads are dominated by internal gains. The savings associated with the thermal mass control strategies would be less and would show more climatic dependence for buildings with more ambient coupling. It should also be noted the strategies only involved mechanical precooling and did not incorporate precooling through use of nighttime ventilation. A building in a dry and hot climate like Phoenix's could benefit significantly from nighttime ventilation.

Typically, utility rates vary according to region and it is difficult to separate climatic and utility effects. Typical rate structures were obtained for the five chosen locations (Boston, Chicago, Miami, Phoenix, and Seattle) and used to carry out simulation studies to analyze the overall impact of location on the savings potential for use of building thermal mass. Table 7 gives the different utility rate structures used for each location. The simulations were carried out using the models obtained for the field site building and equipment.

As illustrated in Table 7, Boston has very favorable utility rates for use of building thermal mass with a very high demand rate, a very low off-peak energy rate, and a high on-to-off peak

Table 7. Comparison of Utility Rate Structures for Different Locations

City	Energy, c/kWh		Energy Cost Ratio	Demand, $/kW	Peak Hours
	Off-Peak	On-Peak		On-Peak	
Boston	0.6	2.9	4.7	18.87	9 A.M. to 10 P.M.
Chicago	2.3	5.2	2.3	16.41	9 A.M. to 10 P.M.
Miami	1.1	2.8	2.5	6.25	12 A.M. to 9 P.M.
Phoenix	2.7	5.1	1.9	14.82	11 A.M. to 9 P.M.
Seattle	3.2	3.2	1.0	1.46	6 A.M. to 10 P.M.

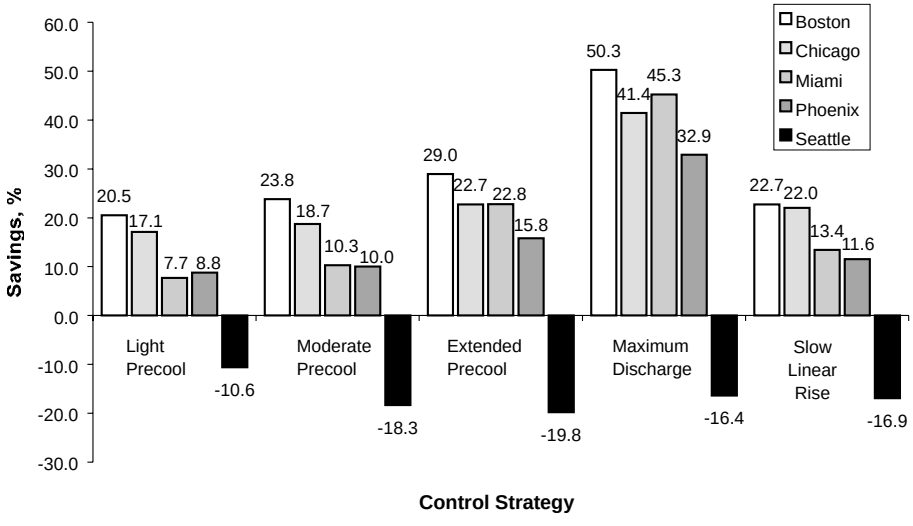

Figure 17. Regional Comparison of Savings Potential of Different Control Strategies

ratio. The length of the peak period is 11 h. At the other extreme, Seattle has a very low demand rate and on-to-off peak ratio and a very long on-peak period (16 h). Chicago has high demand rates and a moderately high on-to-off peak ratio. Miami has moderate demand rates, a moderate on-to-off peak ratio, and a short on-peak period (9 h). Phoenix has a moderate demand rate, a moderately high on-to-off peak ratio, and a relatively short on-peak period (10 h).

Figure 17 gives air conditioning utility cost savings estimates associated with each strategy and location, determined using the appropriate utility information given in Table 7. Savings were achieved in all locations except for Seattle. The greatest savings (50%) were associated with the maximum discharge strategy implemented in Boston. Similar savings were achieved in Chicago and Miami, with some lower savings in Phoenix. The negative savings in Seattle means that night setup is the best strategy for this location. A greater penalty is associated with greater precooling in Seattle. However, night ventilation was not considered in this study. The use of night ventilation could result in some savings for precooling in Seattle.

Table 8 shows a breakdown of costs for the different control strategies in Boston. The overall costs are somewhat similar to the results previously presented for Chicago. However, the demand costs are an even larger portion of the total bill than in Chicago. In addition, Boston has higher on-to-off peak energy ratios and, as previously noted, has a more favorable climate for savings.

Table 8. Energy, Demand, and Total Costs Under Different Control Strategies (Boston)

Strategy	Energy, $	Demand, $	Total, $
Night setup	47,518	2114,275	261,792
Light precool	40,180	167,955	208,135
Moderate precool	37,798	161,709	199,507
Extended precool	35,413	150,569	185,982
Maximum discharge	28,324	101,881	130,205
Slow linear rise	32,032	170,254	202,286

Table 9. Energy, Demand, and Total Costs Under Different Control Strategies (Miami)

Strategy	Energy, $	Demand, $	Total, $
Night setup	62,306	86,172	148,478
Light precool	57,718	79,337	137,055
Moderate precool	56,533	76,696	133,229
Extended precool	53,786	60,854	114,641
Maximum discharge	45,814	35,469	81,283
Slow linear rise	41,172	77,383	128,554

Table 10. Energy, Demand, and Total Costs Under Different Control Strategies (Phoenix)

Strategy	Energy, $	Demand, $	Total, $
Night setup	139,602	199,844	339,446
Light precool	132,582	177,073	309,656
Moderate precool	131,756	173,712	305,468
Extended precool	129,630	156,129	285,759
Maximum discharge	119,079	108,655	227,734
Slow linear rise	127,801	172,421	300,222

Table 9 shows cost breakdowns for the strategies in Miami. Although Miami has much lower demand costs than Boston and Chicago, the relative savings are comparable for the extended precool and maximum discharge strategies (see Tables 6 and 8). However, the light and moderate precool strategies give much smaller savings for Miami than for Boston and Chicago. These trends occur because of differences in when the on-peak period begins. In Miami, the on-peak period does not begin until noon, whereas it starts at 9 A.M. in Boston and Chicago. Strategies that do not maintain the cool building thermal mass during the occupied, on-peak period (light and moderate precool) do not perform well in Miami. For these strategies, the bulk of the load shifting occurs during off-peak hours. The extended precool, maximum discharge, and linear rise strategies all maintain the zone temperature at the lower limit of comfort until the on-peak period begins. The slow linear rise strategy gives much smaller savings for Miami than for Boston or Chicago (see Figure 17). For Miami, the linear rise occurs over a smaller time interval (noon until 5 P.M.) than for Boston and Chicago (9 A.M. until 5 P.M.) so that the mass is not discharged as completely.

Table 10 gives cost breakdowns for Phoenix. Despite a high demand rate and a relatively short on-peak period, relative savings in Phoenix are significantly smaller than in Boston, Chicago, and Miami for all of the control strategies (see Figure 16). As previously explained, this is because the envelope loads and total loads are larger. However, the absolute dollar

Table 11. Energy, Demand, and Total Costs Under Different Control Strategies (Seattle)

Strategy	Energy, $	Demand, $	Total, $
Night setup	51,537	14,881	66,417
Light precool	60,613	12,824	73,436
Moderate precool	66,113	12,486	78,599
Extended precool	66,761	12,782	79,543
Maximum discharge	64,450	12,834	77,284
Slow linear rise	64,774	12,883	77,657

savings associated with any of the control strategies for Phoenix are comparable to those for Boston and Chicago and greater than those for Miami.

Table 11 gives the cost breakdowns for Seattle. The lowest total costs are associated with night setup control. The thermal mass strategies do result in demand cost savings, but these savings are outweighed by increases in energy costs. Energy costs increase with precooling because the off-peak rates are the same as the on-peak values and precooling increases the total cooling loads due to greater envelope gains. Furthermore, the demand savings are relatively small because of the low on-peak demand rate. The best control strategy for Seattle is night setup.

CONCLUSIONS

The cost savings potential for use of building thermal mass can be very significant. However, the savings depend upon utility incentives, building construction, climate, and the type of air conditioning system. The tool presented in this paper is useful for evaluating the savings potential for a particular application and for developing a site-specific control strategy. Models are trained using short-term data and then are used to predict the costs for alternative control strategies. The approach was validated through comparisons of predicted air-conditioning costs with an actual utility bill for one month in the middle of summer for a commercial building located near Chicago. The predictions were within 5% of the utility bill.

The simulation tool was then used to study the performance of alternative control strategies that could take advantage of building thermal mass for load shifting and peak load reduction at the field site. Up to about 40% savings in total cooling costs are possible at the facility in Chicago with strategies that adjust the zone temperature setpoints during both the on-peak and off-peak periods. About 20% savings could be achieved with other strategies that maintain the setpoint in the middle of the comfort range during the on-peak, occupied period.

Similar savings were estimated for the same facility if it were located in Miami, with slightly smaller savings in Phoenix and larger savings in Boston. However, night setup control was found to be the best strategy for Seattle. The utility rates considered in Seattle did not incorporate time-of-use energy charges and had relatively low demand rates. However, the study did not consider the possibility of free cooling during nighttime. The use of free cooling could increase the savings potential for many of the locations considered.

Most of the earlier studies focused on comparisons of cooling load shifting and peak reduction and did not estimate cost savings. Although Braun (1990) presented cost savings similar to those presented in this study, the savings were estimated for a set of hypothetical buildings and the savings were only estimated for single-day simulations. The results in this paper are the first demonstration of seasonal cost savings for an actual facility. Additional work should be performed to demonstrate savings for other field sites.

ACKNOWLEDGMENTS

The work presented in this paper was sponsored by ASHRAE through TC 4.6. We appreciate the direction and patience of the project monitoring subcommittee: John Seem, Rich Hackner, and Frank Mayhew. We also thank Lynn Jester for his efforts in supporting the field testing.

NOMENCLATURE

a_i	model parameters
$c_{p,a}$	specific heat of air
$c_{p,w}$	specific heat of water
C_{tot}	total monthly utility cost [$]
C_z	capacitance associated with internal zone mass (air and furnishings)
e_k	transfer function coefficient for the zone sensible load for k timesteps prior to the current time t
h_a	ambient air enthalpy at current hour
h_z	zone air enthalpy at current hour
$\dot{m}_{sup}$	required zone supply mass flow rate at current hour
$\dot{m}_{vent}$	ambient ventilation air mass flow rate requirement at current hour
$N_{ahu,pairs}$	total number of paired air handling units
$N_{chill,on}$	number of active chillers
$N_{ct,\ fan,\ on}$	number of active cooling fan towers
N_{on}	number of on-peak hours in the simulated month
N_{off}	number of off-peak hours in the simulated month
$P_{AHU,i}$	AHU power consumption at hour i
$P_{ahu,pair}$	total power consumption for paired AHUs
$P_{ahu,total}$	total AHU power
P_{ch}	total chiller power consumption
$P_{CHW,pump}$	individual chilled water pump power consumption
$P_{ct,fan}$	individual cooling tower fan power consumption
$P_{CW,pump}$	individual condenser water pump power consumption
P_{plant}	total plant power consumption
$P_{plant,i}$	cooling plant power consumption at hour i
$P_{tot,i}$	total HVAC power consumption at hour i
$\dot{Q}_{ch,i}$	individual loading of each chiller
$\dot{Q}_{plant}$	total plant cooling load at current hour
$\dot{Q}_{vent}$	ventilation load at current hour
$\dot{Q}_{sh}$	rate of heat gain to the air from the structure
$\dot{Q}_{zl}$	zone latent load at current hour
$\dot{Q}_{zs}$	zone sensible load at current hour
$R_{off,peak}$	off-peak energy rate charge, $/(kWh)
$R_{on,peak}$	on-peak energy rate charge, $/(kWh)
$R_{demand,on}$	demand rate charge, $/(kWh)
$\vec{S}_k$	vector containing transfer function coefficients for the input vector k timesteps prior to current time t
$T_{CHWR,i}$	temperature of the water returning from the building to chillers in pair i
T_{chws}	chilled water supply temperature
$T_{CHWS,unit\ \#1,i}$	temperature of the supply water leaving chiller #1 in pair i
$T_{CHWS,unit\ \#2,i}$	temperature of the supply water leaving chiller #2 in pair i
$T_{ret,i}$	return air temperature in air handler pair i
T_{sup}	supply air temperature to zone
$T_{sup,j}$	supply air temperature in air handler pair i
T_{wb}	ambient wet-bulb temperature
$\vec{u}$	vector of inputs
$\dot{v}_{CHW,unit\ \#1,\ i}$	volumetric water flow rate of chiller unit #1 in pair i
$\dot{v}_{CHW,unit\ \#2,\ i}$	volumetric water flow rate of chiller unit #2 in pair i
$\dot{v}_{pairs,AHU}$	volumetric flow rate through each paired AHU at current hour
$\dot{v}_{sup}$	required zone supply volumetric flow rate at current hour
$\dot{v}_{sup,pair}$	volumetric flow rate for the paired AHU supply fans
$\dot{v}_{sup,pair,i}$	total volumetric airflow rate in air handler pair

Greek

$\Delta\tau$	time step
ρ_a	density of air
ρ_w	density of water

REFERENCES

Andresen, I. and M.J. Brandemuehl. 1992. Heat Storage in Building Thermal Mass: A Parametric Study. *ASHRAE Transactions* 98(1).

ASHRAE. 1997. *1997 ASHRAE Handbook—Fundamentals.* American Society of Heating, Refrigerating, and Air-Conditioning Engineers, Inc. Atlanta, Georgia.

Braun, J.E. 1990. Reducing Energy Costs and Peak Electrical Demand Through Optimal Control of Building Thermal Storage. *ASHRAE Transactions* 96(2):876-888.

Chaturvedi, N. 2000. Analytical Tools for Dynamic Building Control. *Report No. HL2000-15,* Herrick Laboratories, Purdue University, West Lafayette, Indiana.

Chaturvedi, N. and J.E. Braun. 2002. A Robust Inverse Model for Transient Building Loads. Submitted to the *International Journal of Heating, Ventilating, Air-Conditioning and Refrigerating Research* (to appear in January 2002 issue of the *Journal*).

Coniff, J.P. 1991. Strategies for Reducing Peak Air Conditioning Loads by Using Heat Storage in the Building Structure. *ASHRAE Transactions* 97:704-709.

Golneshan, A.A. and M.A. Yaghoubi. 1990. Simulation of Ventilation Strategies of a Residential Building in Hot Arid Regions of Iran. *Energy and Buildings* 14:201-205.

Keeney, K.R. and J.E. Braun. 1997. Application of Building Precooling to Reduce Peak Cooling Requirements. *ASHRAE Transactions* 103(1):463-469.

Montgomery, K.W. 1998. Development of Analysis Tools for the Evaluation of Thermal Mass Control Strategies. *Report* No. HL98-17, Herrick Laboratories, Purdue University, West Lafayette, Indiana.

Morris, F.B., J.E. Braun, and S.J. Treado. 1994. Experimental and Simulated Performance of Optimal Control of Building Thermal Storage. *ASHRAE Transactions* 100(1):402-414.

Rabl, A. and L.K. Norford. 1991. Peak Load Reduction by Preconditioning Buildings at Night. *International Journal of Energy Research* 15:781-798.

Ruud, M.D., J.W. Mitchell, and S.A. Klein. 1990. Use of Building Thermal Mass to Offset Cooling Loads. *ASHRAE Transactions* 96(2):820-829.

Snyder, M.E. and T.A. Newell. 1990. Cooling Cost Minimization Using Building Mass for Thermal Storage. *ASHRAE Transactions* 96(2):830-838.